Modeling the vegetation dynamics of northern shrubs and mosses in the ORCHIDEE land surface model

Arsène Druel, Philippe Ciais, Gerhard Krinner, Philippe Peylin

HAL Id: hal-02398277
https://hal.science/hal-02398277

Submitted on 17 Sep 2020

Modeling the Vegetation Dynamics of Northern Shrubs and Mosses in the ORCHIDEE Land Surface Model

Arsène Druel[1,2,3] iD, **Philippe Ciais[2]** iD, **Gerhard Krinner[1]** iD, and **Philippe Peylin[2]** iD

[1]CNRS, Université Grenoble Alpes, Institut des Géosciences de l'Environnement (IGE), Grenoble, France, [2]Laboratoire des Sciences du Climat et de l'Environnement, CEA-CNRS-UVSQ CE Orme des Merisiers, Gif sur Yvette, France, [3]Now at CNRM-Université de Toulouse, Météo-France, CNRS, Toulouse, France

Abstract Parameterizations of plant competition processes involving shrubs, mosses, grasses, and trees were introduced with the recently implemented shrubs and mosses plant functional types in the ORCHIDEE dynamic global vegetation model in order to improve the representation of high latitude vegetation dynamics. Competition is based on light capture for growth, net primary productivity, and survival to cold-induced mortality during winter. Trees are assumed to outcompete shrubs and grasses for light, and shrubs outcompete grasses. Shrubs are modeled to have a higher survival than trees to extremely cold winters because of thermic protection by snow. The fractional coverage of each plant type is based on their respective net primary productivity and winter mortality of trees and shrubs. Gridded simulations were carried out for the historical period and the 21st century following the RCP4.5 and 8.5 scenarios. We evaluate the simulated present-day vegetation with an observation-based distribution map and literature data of boreal shrubs. The simulation produces a realistic present-day boreal vegetation distribution, with shrubs, mosses north of trees and grasses. Nevertheless, the model underestimated local shrub expansion compared to observations from selected sites in the Arctic during the last 30 years suggesting missing processes (nutrients and microscale effects). The RCP4.5 and RCP8.5 projections show a substantial decrease of bare soil, an increase in tree and moss cover and an increase of shrub net primary productivity. Finally, the impact of new vegetation types and associated processes is discussed in the context of climate feedbacks.

Plain Language Summary Changes in the northern vegetation exert feedbacks on climate through surface energy and greenhouse gas fluxes. For example, increased vegetation cover can lead to warming due to stronger absorption of shortwave radiation (through decreased albedo). In this study we developed a new version of the ORCHIDEE dynamic vegetation model, allowing us to simulate the dynamical cover of mosses and shrubs, two important types of northern vegetation, alongside with grasses and trees. The prevalence of the different forms of vegetation is ruled by light capture during the growing season, mortality during the cold conditions, and competition for space. The new model is tested for present-day land cover and used for future climate projections. We simulated a realistic vegetation map for historical simulations and a substantial decrease of bare soil with shifts of vegetation in future simulations. However, the model underestimated local shrub expansion compared to observations.

1. Introduction

Earth system models (ESMs) with integrated land surface models (LSMs) are used for projections of vegetation changes in conjunction with climate change (Cox et al., 2000; Oki & Kanae, 2006; Piao et al., 2006; Schimel, 1995; Trenberth et al., 2009). It is essential to take into account and to be able to project vegetation changes in ESMs because during large climate shifts the feedbacks of vegetation on climate can be very strong. This was the case during the Last Glacial Inception (approximately 11,5000 years before present), which was correctly reproduced in climate models only when shifts in vegetation distribution were taken into account using dynamic global vegetation models (DGVMs; Crucifix & Loutre, 2002; Gallimore & Kutzbach, 1996; Meissner et al., 2003; de Noblet et al., 1996; Quillet et al., 2010). Recent climate feedbacks from vegetation changes were also demonstrated (Lawrence & Swenson, 2011; Loranty et al., 2014; Luus et al., 2013; Pearson et al., 2013; Porada et al., 2016), such as a consistent decline of albedo with increasing tree cover (Loranty et al., 2014). High-latitude ecosystems have a significant impact on the climate (Bonan, 1995; Chapin et al., 2000; Christensen et al., 1999), for example, the increase of annual temperature at regional scales due to shrub cover increase (Bonfils et al., 2012). Yet shrub expansion is observed in many Arctic

areas (Myers-Smith et al., 2011; Naito & Cairns, 2015; Sturm, Holmgren, et al., 2001; Tape et al., 2006) and is attributed to the ongoing changes in climate (e.g., to changes in annual precipitation in Frost & Epstein, 2014). The vegetation distribution change contributes to the observed increase of leaf area in the Arctic (Blok, Schaepman-Strub, et al., 2011; Bonfils et al., 2012; Elmendorf et al., 2012; Jiang et al., 2012; Xu et al., 2013).

In the majority of DGVMs, vegetation competition and disturbances are implemented at a daily to yearly time step (Krinner et al., 2005; Sitch et al., 2003). The representation of vegetation competition usually includes competition for light, and vegetation extension on free space often depends on their relative primary productivity (Krinner et al., 2005; Prentice & Leemans, 1990; Sitch et al., 2003). Disturbances and bioclimatic factors, such as fires, frost (Pachzelt et al., 2015; Sinclair et al., 2007; Thonicke et al., 2008), herbivory, or trampling (Gill, 2014; Olofsson et al., 2009; Zimov et al., 1995), drive vegetation mortality and productivity and, consequently, competition among plant types and their distribution (Haxeltine & Prentice, 1996; Prentice et al., 1992). In northern latitudes the vegetation is particularly sensitive to temperature, because an increase of temperature above 0 °C can lengthen the growing season and decrease mortality due to extreme cold conditions. These interactions can have impacts on physical variables such as the albedo (Brovkin et al., 2003; Cook et al., 2008; Foley et al., 1994; Meissner et al., 2003), which changes significantly if vegetation is above or below the snow. Vegetation also affects soil thermal properties, by affecting snow thickness and thus thermal insulation by snow cover (Liston et al., 2002), by low conductivity moss and lichen layers (Chadburn et al., 2015b; Porada et al., 2016), and by the presence of soil organic carbon (Epstein et al., 2000; Koven et al., 2011; Rinke et al., 2008). Thus, vegetation shifts will change the carbon balance of ecosystems, the surface energy budget, and the soil thermic and hydrological regimes (Betts, 2000; Cox et al., 2000; Zhang et al., 2013), for instance, snow-season albedo, soil moisture, or evapotranspiration in former grasslands transformed into forests. These processes can lead to positive or negative feedbacks on temperature (Foley et al., 1994). Nowadays, many DGVMs contain a description of shrubs, such as in the Community Land Model (Oleson et al., 2013), mosses, or both, such as in BIOME4 (Kaplan et al., 2003), JULES (Chadburn et al., 2015a; Clark et al., 2011), and JSBACH (Baudena et al., 2015; Porada et al., 2013, 2016).

In order to be able to simulate the changes of spatial cover of high-latitude vegetation (and thus associated feedbacks), one thus needs to represent the competition for space between shrubs, mosses, trees, and grasses in such regions. For this purpose, a representation of shrubs and mosses had to be incorporated in the DGVM module of a LSM, here ORCHIDEE, including the development of new processes. This modified model is tested for its ability to capture the recent observed Arctic greening and shrub expansion over the last decades. Furthermore, the sensitivity of the simulated vegetation distribution to possible future climate change is explored.

2. Methods

2.1. Overall ORCHIDEE Model Description

We have used ORCHIDEE (Organizing Carbon and Hydrology in Dynamic Ecosystems), the LSM component of the IPSL-CM ESM (Institute Pierre Simon Laplace Climate Model). ORCHIDEE was first described in Krinner et al. (2005), with the vegetation dynamics module directly introduced from the Lund-Potsdam-Jena model (Sitch et al., 2003). The version of ORCHIDEE used in this study (ORC-HL-VEGv1.0, Druel et al., 2017) includes key processes relevant for high latitudes: (i) a soil-freezing scheme and its effect on root water availability and soil thermodynamics in order to represent permafrost (Gouttevin et al., 2012), (ii) an improved snow scheme describing the snow pack with three explicit snow layers (Wang et al., 2013) based on the ISBA-ES LSM (Boone, 2002), and (iii) nonvascular plants (bryophytes and lichens, referred as moss in this article) and shrubs as two new plant functional types (PFTs) compared to the original version of ORCHIDEE, with specific equations and parameters (Table S1). Using a prescribed constant spatial distribution of the PFTs from a satellite land cover map, Druel et al. (2017) analyzed the impact of including these new PFTs on the net and gross carbon fluxes and the surface energy budgets over the boreal and Arctic zone. In this paper, we focus on modeling the dynamic competition of mosses and shrubs with grasses and trees in order to calculate the spatial coverage of each of these PFTs. As a general principle the competition between PFTs (and thus the fractional area occupied by each PFT in a grid box) is based on light access, net primary
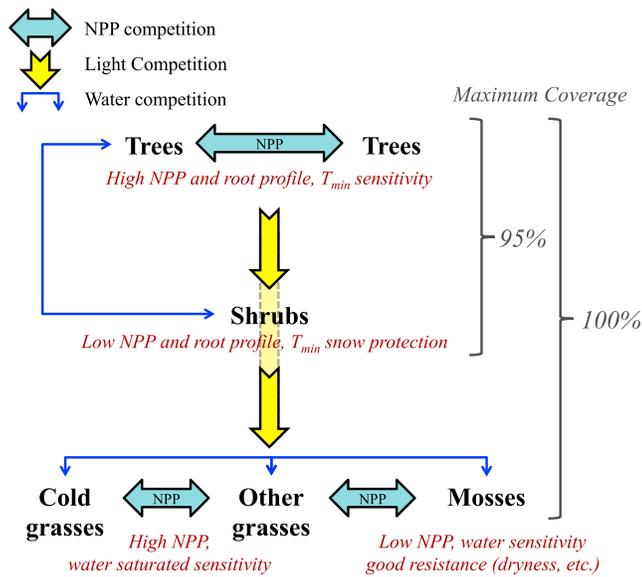
Figure 1. Summary of the main dynamical processes involving boreal vegetation. Thin blue arrows represent the water competition inside a soil tile. The yellow arrow represents the light competition, and its direction indicates the dominated vegetation when the maximum coverage is reached. The wide sky blue arrows represent the competition inside a vegetation layer, based on the plant productivity depending on the plant functional type (PFT) capacities and environmental conditions. Main PFT characteristics influencing the competition are indicated in dark red. Competition between grasses and other grasses or trees and other trees represents the competition between the different PFTs (e.g., cold C3 grasses vs. C4 grasses). NPnet primary productivity.

productivity (NPP), and mortality (depending on climate-related thresholds). There is currently no vertical discretization of the vegetation in ORCHIDEE. Therefore, it is not yet possible in this study to simulate multiple vegetation layers, such as understory vegetation with mosses/grass/shrubs under trees. Note that the dynamical vegetation model in ORCHIDEE, initially described in Krinner et al. (2005), has been revised by Zhu et al. (2015) in order to calibrate the key parameters controlling the vegetation distribution, following the recent model improvements.

2.2. Vegetation Competition

In ORCHIDEE, as long as there is available space (bare soil) and enough water supplies in a grid box, there is no direct competition between PFTs: They can expand if they are adapted to local climatic conditions (i.e., the NPP exceeds the mortality). Three types of processes mainly drive the spatial competition in the modified DGVM of ORCHIDEE (as represented in Figure 1):

1. Water competition occurs for different PFTs present within a given soil tile. There are three different soil tiles, which contain all the herbaceous PFTs, all tree PFTs and bare soil respectively. Shrubs were introduced in the soil tile of trees, while mosses and Arctic grasses were introduced in the herbaceous tile.

2. Direct light competition between PFTs only occurs when the foliage-projected cover (FPC) on the soil approaches 1. When light competition occurs due to space constraints, trees are assumed to receive more light and outcompete grasses and mosses. The grass fraction of a grid cell is then reduced (Krinner et al., 2005; Sitch et al., 2003). Shrubs have an intermediate height and are assumed to outcompete both herbaceous and moss vegetation for light. Therefore, if the woody vegetation FPC defined by shrubs and trees reaches over 0.95, shrubs are dominated by trees and their fractional cover is reduced (through an increase of mortality) until total woody FPC does not exceed 0.95. If the tree FPC exceeds 0.95, the FPC of the remaining trees is reduced to the threshold of 0.95 (see Figure 1). Then, if total FPC (herbaceous and woody vegetation) >1, we increase the mortality of grass and moss PFTs, thereby reducing their fractional cover.

3. Competition within each vegetation layer (herbaceous, shrubs, or trees) is calculated based on the NPP. When the vegetation cover is closed (FPC approaches 1), to comply with (II), the same relative reduction of spatial coverage (through increased mortality) is applied to all PFTs inside a vegetation layer. As a consequence, the most productive PFTs, which grow faster than others, fill up most of the newly available space and gradually outcompete the others. Thus, all factors impacting the NPP (e.g., water stress and desiccation) are able to affect the spatial repartition of PFTs. Conversely, as long as the FPC is low, there is no NPP-based competition: The vegetation types can coexist.

2.3. NPP Control

The NPP can be diagnosed from vegetation respiration and gross primary production. Gross primary production depends on the leaf area index (LAI), temperature, humidity, water availability, and light limitation occurring from Rubisco at low irradiance and from electron transport rate at high irradiance. The Rubisco-limited carboxylation rate is given by the parameter $Vc_{\max(25)}$ at 25 °C and the electron transport limited rate $Vj_{\max}$ is assumed to be proportional to $Vc_{\max}$. The formulation of $Vc_{\max}$ depends upon temperature (Yin & Struik, 2009), with an acclimation to seasonal temperature conditions through the monthly mean temperature as detailed in Druel et al. (2017). Boreal vegetation has a lower $Vc_{\max(25)}$ than standard PFTs (Table S1) and thus lower potential productivity in optimal conditions.

With specific environmental conditions, other variables than temperature control $Vc_{\max(25)}$. For mosses, $Vc_{\max(25)} = 28\ \mu\text{mol}\cdot\text{m}^{-2}\cdot\text{s}^{-1}$ (cf. to 70 $\mu\text{mol}\cdot\text{m}^{-2}\cdot\text{s}^{-1}$ for original grasses) and water stress occurs because of restricted access to soil water (99% of "roots" are considered above 11 cm for mosses vs. 50 cm for C3

grasses), as defined after a calibration of key model parameters with in situ data in Druel et al. (2017). The higher long-term resistance of mosses to soil water stress is due to their ability to dry out and restart as soon as favorable conditions return. This reversible desiccation process was modeled by prescribing a lower mortality rate for mosses and a $Vc_{\max}$ limitation based on a monthly soil moisture stress factor (w_s) rather than a daily/hourly one. The stress factor is defined by the convolution of the moss root fraction in each layer with the relative soil water content (Druel et al., 2017). To take into account the higher water stress of grasses compare to mosses in water-logged soils, we decrease the $Vc_{\max(25)}$ of grasses when the soil is water saturated ($1 \geq w_s > w_{s\_\max}$) by a so-called anoxic factor (a_f) defined by equation (1).

$$
\begin{aligned}
&\text{If} \quad w_s > w_{s\_\max}, \ a_f = a_o + \frac{1 - a_o}{w_{s\_\max}} \times w_s \\
&\text{Else } w_s \leq w_{s\_\max}, \ a_f = 1
\end{aligned}
\tag{1}
$$

Here $w_{s\_\max}$ is a threshold defining water-saturated soil (0.97) and a_0 a minimum anoxic factor equal to 0.2.

In addition, a temperature-dependent reduction of productivity due to frost was added, which indirectly controls in the DGVM the distribution of the temperate and boreal broadleaf deciduous tree PFTs (Zhu et al., 2015).

2.4. Survival Capacity

In cold regions, the most important bioclimatic factor for tree survival is cold temperatures, modeled by a PFT-dependent linearly increasing mortality rate below a critical daily minimum temperature. Furthermore, trees cannot exist if the mean air temperature during the warm season (defined when the minimum temperature of the week is above 0 °C, Zhu et al., 2015) is less than 7 °C. In this study, we set the minimum daily critical air temperature to −45 °C for shrubs, equal to that of boreal needle-leaved evergreen and broadleaved summer green (see Table 1 of Zhu et al., 2015; Table S1).

For shrubs, we adapted the cold-induced mortality as a function of snow thickness. In presence of snow, the minimum temperature ($T_{\min}$) used to calculate tree mortality in the DGVM is the 2-m air temperature, while for shrubs it is based on the snowpack temperature profile (in general warmer), as described in Druel et al. (2017). Therefore, the part of shrubs covered by the snowpack, defined by the snow depth (itself function of snow mass and density) and the shrub height (following shrub specific allometry; see Text S1 in the supporting information), is protected from being exposed to critical daily minimum temperatures by the snow cover.

In order to represent the specific resistance of mosses to drought, a stronger resilience to water stress was assigned to mosses compared to grasses. This reflects their desiccation capacity (leading to a lower mortality), as described in Druel et al. (2017).

2.5. Configuration of Simulations

Simulations of the vegetation distribution at 2° resolution between 40°N and 90°N are presented in this study for the historical period (20th century) and the 21st century with two different RCP scenarios (Moss et al., 2010). Simulations for the historical period use CRUNCEP meteorological forcing (Viovy, 2015; Wei et al., 2014) from 1901 to 2013. The model is spun up for 1,000 years using random forcing years from 1901 to 1950 to equilibrate vegetation distributions in the DGVM (attained after around 250 years) and woody biomass pools.

Sensitivity tests to future climate conditions are based on RCP 4.5 and 8.5 scenarios, corresponding to a radiative forcing of approximately +4.5 and +8.5 W/m^2 in 2100 (Moss et al., 2010). The meteorological forcing is constructed using an anomaly method following Koven et al. (2015), applied to the present-day CRUNCEP forcing and using climate anomalies from the IPSL-CM5 general circulation model simulations (Dufresne et al., 2013). It is provided at a horizontal resolution of 2°, from 2014 to 2100. The initial conditions for the sensitivity tests to future climate conditions are the final vegetation and soil state of the historical simulation.
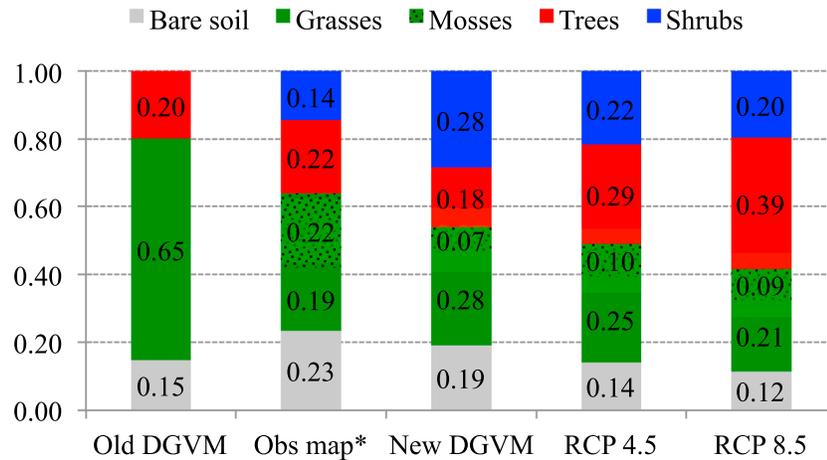
Figure 2. Stacked bar chart of vegetation coverage in northern latitudes (north of 60°N), with on the left a simulation using ORCHIDEE old DGVM (13 PFTs) at present day (between 1984 and 2013), then present-day observation map using satellite data (*from Druel et al., 2017), in the middle present-day (between 1984 and 2013) simulation with the new DGVM (16 PFTs with cold C3 grasses, shrubs, and mosses), and then two simulation for future scenarios (between 2071 and 2100) with RCP 4.5 and 8.5 (right). The value of vegetation fraction cover [0-1] is indicated for each vegetation cover. PFT = plant functional type; DGVM = dynamic global vegetation model.

3. Results

3.1. Present-Day Simulated Vegetation Distribution

Compared to the original DGVM in ORCHIDEE (Krinner et al., 2005), the new one presented here contains three additional PFTs being cold C3 grasses, shrubs, and mosses, as well as new processes associated to these new PFTs. The parameters for trees and other grass PFTs were not modified in the vegetation dynamic module in order to isolate the consequences of the introduction of the new PFTs.

Figures 2 and 3 show the vegetation cover and its distribution at northern latitudes (north of 60°N), averaged for a 30-year period during present-day conditions, from a simulation with the old and new DGVM (1984–2013) and from an observation-based vegetation map used in Druel et al. (2017). This vegetation map combines the satellite-based land cover product of the European Space Agency Climate Change

Figure 3. Composite-color maps of the present-day vegetation coverage in northern latitudes (north of 60°N), with on the left simulation using ORCHIDEE old DGVM (13 PFTs), on the right ORCHIDEE using the new DGVM (16 PFTs with cold C3 grasses, shrubs, and mosses) and in the middle observation map using satellite data (*from Druel et al., 2017). Both simulated maps show mean between 1984 and 2013. Color coding is such that saturation indicates total grid-scale coverage maximum (=1), while hue indicates the relative vegetation coverage following the three vegetation layers: woody vegetation in red (only trees with the old DGVM simulation - trees and shrubs otherwise) and herbaceous in green (including C3 and C4 standard grasses with the old DGVM simulation, and with cold C3 grasses and mosses in addition otherwise). PFT = plant functional type; DGVM = dynamic global vegetation model.

Initiative (available at http://www.esa-landcover-cci.org/), the Circumpolar Arctic Vegetation Map (CAVM Team, 2003), and the map developed by Loveland et al. (2000). Comparing with the observation-based map, the two simulations tend to have more land covered predominantly with one type of vegetation (fractional cover close to 1; i.e., saturated colors). Notably, the tree cover is overestimated in Europe and West Asia in both simulations. The herbaceous coverage is overestimated in most parts of North America and East Asia in the old DGVM, while the shrub cover in the new DGVM is overestimated on a smaller area in West America and extreme East Asia. However, compared to the observation-based vegetation map (36%), the present-day simulated woody cover is closer to the new DGVM (46%) than to the old DGVM (20%), despite a suspected overestimation of shrubs. The old DGVM also clearly underestimates such cover. Moreover, the woody cover simulated with the new DGVM is more widely distributed, and its distribution better fits that of the observation-based estimate. The simulated herbaceous cover is also closer to the observations with the new DGVM; we obtain a mixture of vegetation cover (dark green color in Figure 3), when there is mainly herbaceous dominance (light green) with the old DGVM.

The introduction of the new PFTs does not substantially change the tree distribution compared to the standard DGVM. Tree coverage is slightly reduced, from 20% to 18% on average, versus 22% in the observation-driven map. Trees are not impacted much by adding shrubs in the DGVM, because they outcompete them through competition for light, and small differences in tree cover with the new DGVM (see Figure S1) can only be due to the competition for water. In areas devoid of trees, according to the observation-driven map, shrubs are growing reasonably well in the new DGVM version, which leads to an average coverage of 28% north of 60°N. Such growth is due to the shrub resistance to extreme frost condition (through snow protection). This increased shrub cover occurs at the expense of grasslands due to the light competition, resulting in a drastic grass cover reduction from 65% to 28%. Compared to the present-day vegetation map, this smaller new DGVM grass coverage is more realistic (19% in the observation-based map). In the new DGVM, the mosses occupy 7% of the high-latitude area at the expense of grasses. However, such moss cover is still lower than in the observation-based vegetation map, with a moss fraction of 22%.

In summary, the new DGVM matches better the observation-based vegetation distribution, and the new PFTs introduced in the DGVM let shrubs extend further poleward than trees. This allows simulating shrub tundra north of the taiga belt, although the simulated coverage (28%) seems too high compared to the observation-based map (14%). This difference is mainly due to regional biases, particularly in East Siberia or Western North America, highlighted with a saturated red color in the new DGVM map in Figure 3, where the simulated shrub fraction is around 100% while it does not reach 50% in the reference map. However, one has to keep in mind that the observation-based map relies primarily on satellite land cover maps that have large uncertainties, as discussed in Hartley et al. (2017).

3.2. Future Evolution of the High-Latitude Vegetation

In order to assess the model behavior and sensitivity with the newly implemented vegetation in this DGVM, some projections were made with different scenarios. Figures 2 and 4 show the simulated vegetation fractional cover and spatial distribution in northern latitudes (north of 60°N) with the new DGVM, averaged for two 30-year periods: present-day (1984–2013) and end of this century (2071–2100). There is a global reduction of herbaceous and shrubs cover over time from 1984–2013 to 2071–2100 in favor of trees, which expand their distribution area to the north (by +65% in RCP 4.5 and +220% in RCP 8.5 north of 60°N) very similarly to the tree expansion with the old DGVM (see Figure S1). However, no noticeable expansion of coverage is observed for shrubs, herbaceous plants, and mosses, which altogether remain confined to the current range. To investigate the full temporal evolution of the vegetation time series, 15-year smoothed vegetation coverage for three latitudinal bands is presented in Figure 5. Spin-up starts without vegetation (100% bare soil) and gradually PFTs expand along spatial gradients in environmental conditions. While for shrubs and grasses 25 years are enough to stabilize their coverage, mosses require up to 50 years, and trees take more than 200 years (≈250 years in most grid cells). We found that where trees dominate at equilibrium under preindustrial climate (south of 75°N), there is a transient regime during spin-up. Initially, shrub and grass covers increase to reach their maximum after 20 to 30 years, after which trees take over (Figure 5c). Where shrub cover dominates under equilibrium, a similar transient behavior is observed, with shrub cover attaining its maximum after grasses. This behavior reflects slow changes in the balance between light competition favoring woody vegetation and the occurrence of very cold winters killing trees and shrubs
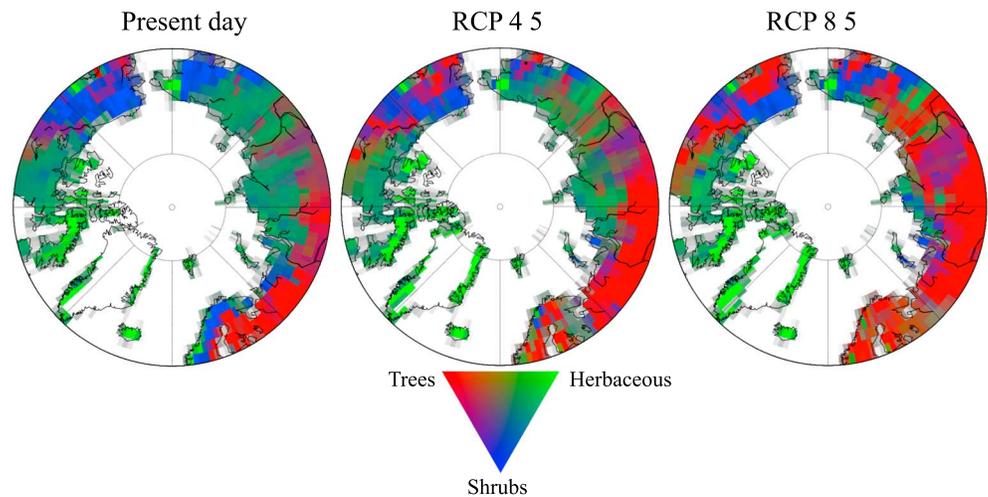
Figure 4. Composite-color maps of the simulated annual vegetation coverage in northern latitudes (north of 60°N), with the new dynamic global vegetation model (16 plant functional types with cold C3 grasses, shrubs, and mosses) using three scenarios: on the left present day (between 1984 and 2013), in the middle and on the right future scenarios (between 2071 and 2100), respectively RCP 4.5 and RCP 8.5 (right). Color coding is such that saturation indicates total grid-scale coverage maximum (=1), while hue indicates the relative vegetation coverage following the three vegetation layers: trees (red), shrubs (blue), and herbaceous (green, including C3 and C4 standard grasses, cold C3 grasses and mosses).

occasionally (section 2.2). Between 1901 and 1950, the vegetation is very stable, as the spin-up was computed by repeating forcing years of this period randomly. Then, from 1950 to 2000, changes progressively appear in some pixels, but at the scale of whole latitudinal bands these local changes compensate for each other. After 2000, however, more uniform changes emerge in each latitudinal band, and amplify in the end of this century.

In the boreal band (55°N to 65°N), moss and grass cover (respectively 2.7% and 20.1% in 1984–2013) remain almost constant over time, while tree coverage (38% in 1984–2013) starts to increase after the 2000s and reaches up to +42% (over present days) for RCP 4.5 and +68% for RCP 8.5 (in 2071–2100). Shrub coverage decreases in parallel (respectively by −32% and −56% from the 33% mean coverage in 1984–2013).

In the Arctic band (65°N to 75°N) the present-day maximum coverage reached by shrubs (29%) and trees (10%) is lower than in the boreal band, while there are more grasses (34%) and mosses (8% in 1984–2013). Generally, future changes in the different vegetation layers are lower than in the boreal band, except for trees. The relative coverage of trees increases between +120% for RCP 4.5 and +230% for RCP 8.5 at the expense of shrubs (respectively −18% and −20%) and grasses (respectively −9% and −27%).

For the very high latitudes (north of 75°N) the equilibrium takes more time to establish. For the present day a predominant coverage of mosses (16.8%), only a few shrubs (3.9%), less grasses (12.2%) than for other latitudes, and no tree fraction are simulated. Relatively small change with time is simulated in this band for shrubs (+14% for RCP 4.5 and +33% for RCP 8.5). However, grasses increase consequently (respectively by +58% and +89%), as well as mosses (+56% and +62%). As a result, there is a considerable decrease of bare soil coverage from 67% in 1984–2013 to 50% (−26%) with RCP 4.5 and 44% (−34%) with RCP 8.5 in 2071–2100. Mosses become the largest vegetation cover in the future above 75°N, followed by grasses (including cold C3 grasses), indicating a very good adaptation of mosses to extreme climate, in spite of the very strong annual mean surface air temperature increase of about +9 °C in this latitude band by 2100 in RCP 8.5 (+5 °C in RCP 4.5). In southernmost latitudes, trees seem particularly sensitive to climate warming and they can become dominant in boreal latitudes (55°N to 65°N).

3.3. Shrub Dynamics at Site Locations With Shrub Cover Change Observations

To compare the modeled shrub dynamics, we selected several Arctic sites where shrub cover change has been documented over the last decades from field data and high-resolution remote sensing images. Here we chose to compare not only modeled shrub cover but also the LAI and the NPP with observed shrub cover. Indeed,
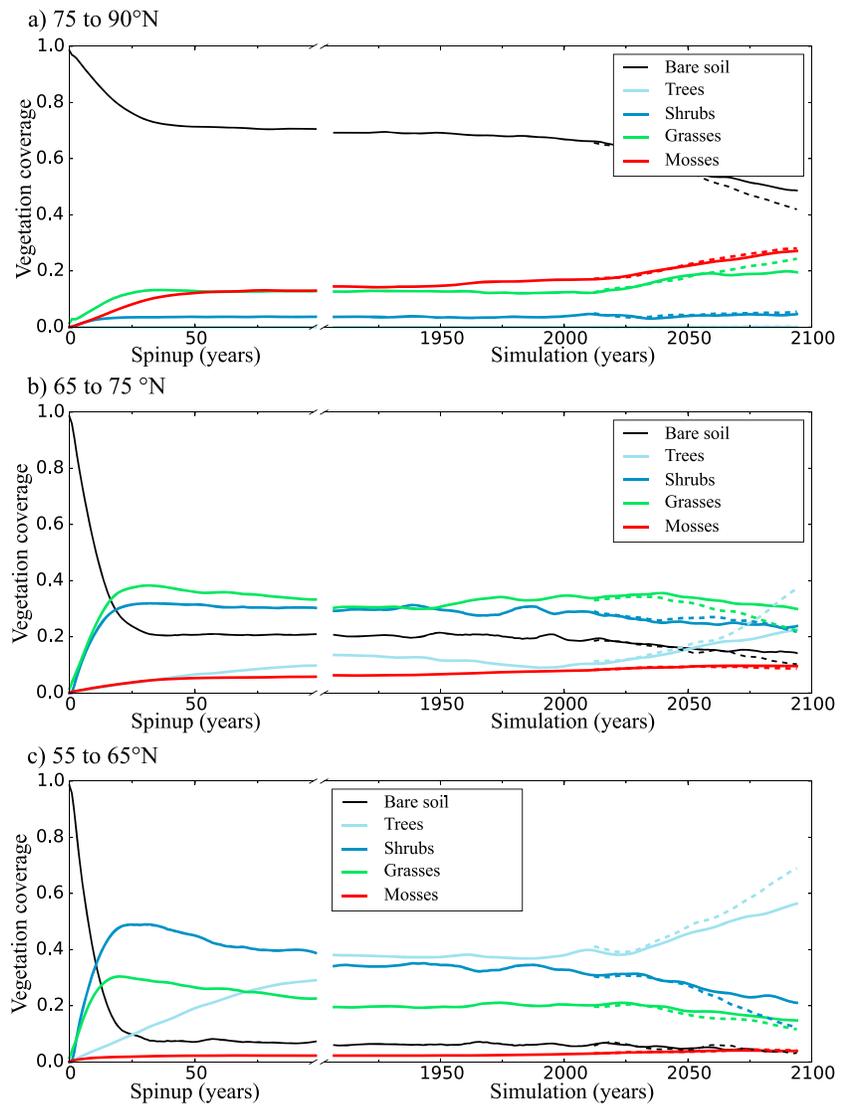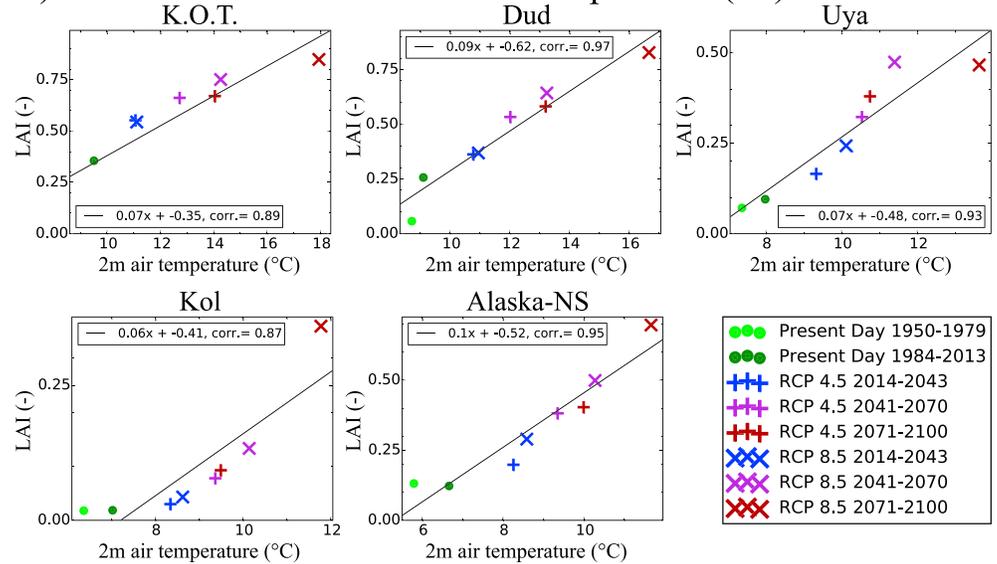
Figure 5. Time series of 15-year smoothed maximum vegetation coverage in (a–c) three different latitudinal bands (55°N to 65°N, 65°N to 75°N, and above 75°N), with the first 100 years of spin-up (from 1,000 years), the present-day simulation (1901 to 2013), future (2014 to 2100) RCP 4.5 simulation (solid line), and future RCP 8.5 simulation (dotted line). PFT = plant functional type.

the coarse resolution of our simulations does not allow a "like for like" comparison with site data where shrub changes are highly heterogeneous and occur at microscale (Cresto Aleina et al., 2015) and can be due to other than climatological factors such as nutrient limitations (Macias-Fauria et al., 2012; see their Figure 1). Figure 6 shows annual mean shrub LAI simulated at the selected locations. The first four locations include six sites used in Frost and Epstein (2014): K.O.T. (containing the three sites Kharp, Obskaya and Tanlova), Dudinka, Uyandi, and Kolyma. The last location (Alaska-NS) is situated in the north slope of Alaska and contains all sites presented in Tape et al. (2006).

As expected from numerous studies (Bull, 1968; Lane et al., 2000; Öztürk et al., 2015; Zhang et al., 2002), the model results show a high positive correlation (from 0.76 to 0.97) between shrub LAI and summer air temperature or annual precipitation for all locations. The results are very similar for NPP (Figure S2) with positive correlations from 0.74 to 0.98 and an increase over time.

Table 1 compares the relative trend of modeled shrub cover and LAI with that of observed shrub cover change and the observed and simulated recent shrub cover. First, as noticed above, the simulated shrub cover is much larger than observed at all sites, except Dudinka. Likewise, the simulated shrub cover has
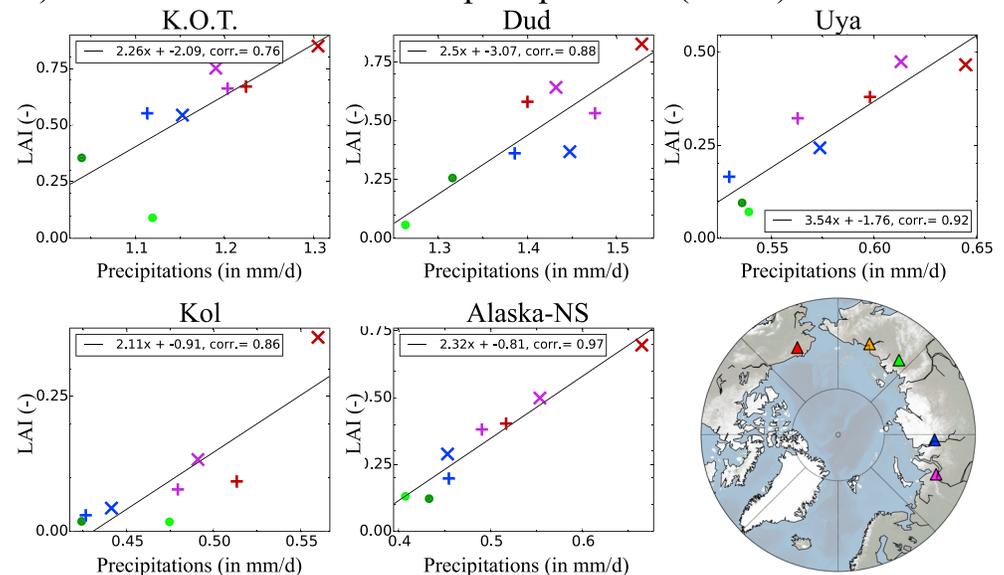
Figure 6. Shrub mean annual leaf area index (LAI) simulated as a function of (a) air temperature (°C) in summer (July/August/September) and (b) annual precipitation (mm/day) for five locations and five periods. The five locations are presented on the map, with in northern Siberia K.O.T (for Kharp, Obskaya, and Tanlova) in magenta (66–68°N, 66–70°E), Dudinka in blue (68–70°N, 86–88°E), Uyandi in green (68–70°N, 140–142°E), Kolyma in orange (68–70°N, 160–162°E), and with Alaska North Slope in red (68–70°N, 162–142°W).

no clear temporal variation across all sites (on average −0.22% per year with a standard deviation [SD] of 0.95%), while the observed cover increases slightly but significantly over time (0.43% per year with SD = 0.14%). For the model, the very large SD poses some questions with respect to the interpretation of the mean trend; it suggests primarily that some drivers of the observed shrub cover changes are not currently modeled (e.g., fire, nutrient limitation, soil heterogeneity, and wind stresses; see section 4). In parallel, modeled shrub LAI increased on average by 1.8% per year (SD = 2.19%) between 1950–1979 and 1984–2013, with a range between −0.2% at Alaska-NS and 4.4% at Dudinka. Although there is no real trend in the simulated shrub cover at these sites (using the results from the gridded simulations), there is a clear

Table 1
Comparison Between Shrub Cover Change and LAI Evolution Simulated (% per Year Between 1950–1979 and 1984–2013) and Observed Cover Change (% per Year), and Then Shrub Cover Simulated (Between 1984 and 2013) and Cover Presented in Frost and Epstein (2014; Between 1960s and 2000s for K.O.T. (Sites Kharp, Obskaya, and Tanlova), Dudinka, Uyandi, and Kolyma) and in Tape et al. (2006; between 1965–1968 and 2002–2011)

Site	Simulated cover change (% per year)	Simulated LAI evolution (% per year)	Observed cover change (% per year)	% cover simulated (1984–2013)	% Cover observed (2000s)
K.O.T.	−1.3%	4.0%	0.38%	38%	11%
Dudinka	−0.98%	4.4%	0.58%	27%	32%
Uyandi	0.11%	0.83%	0.33%	36%	0.04%
Kolyma	0.00%	0.13%	0.27%	36%	7.5%
Alaska-NS	1.1%	−0.20%	0.57%	88%	20%

Note. LAI = leaf area index; K.O.T = Kharp, Obskaya, and Tanlova.

increase of shrub cover in observation, which is somehow mirrored in the model by an increase of the simulated LAI (with larger values but a less pronounced trend). It is however difficult to compare LAI changes with plant cover changes, although in both cases an increase is commonly attributed to favorable conditions. At Dudinka or K.O.T., the model LAI increase correlates with the observed strong increase in shrub cover, while the simulated shrub cover slightly decreases. At Alaska-NS the simulated small decrease of LAI occurs with a substantial increase of cover change, reaching a very high shrub cover (88%) compared to the observations (increase of 0.57% per year to reach 20%). In our sensitivity tests to future climate change, in the RCP 4.5 scenario the simulated LAI increase in 2100 is slightly higher but more homogeneous in between sites than in the present-day simulation, with a mean of 1.3% (SD = 0.46%) and a range between 0.73% and 1.9% per year. Under the RCP 8.5, the shrub LAI increase is slightly more pronounced (1.94% with SD = 0.94%). The scenario with higher temperature and precipitation changes induces large differences in the shrub productivity, revealed by large LAI changes, although the fraction of the vegetation cover does not change much.

4. Discussion

4.1. Present-Day Simulated PFT Distribution

The results shown above reflect closely the theoretical assumptions made in the DGVM (sections 2.2 to 2.4). The inclusion of mosses and shrubs has a limited impact on the spatial distribution of trees (Figures 2, 3, and S1) given that competition for light always favors trees (section 2.2). The slight decrease of tree coverage can be attributed to soil water competition with shrubs, due to the fact that they share the same soil water tile. Shrub and tree mortality from minimum winter temperatures is a key parameter in our simulation, and its modification can significantly change the vegetation distribution (as show in Figure S3). However, in this study, we have chosen to focus on the impact of adding new PFTs (mosses and shrubs) without changing the parameterization of the existing PFTs. Another source of uncertainty is the impact of changes in fire regimes, as summers and springs will get warmer and dryer in the boreal region in the future. More intense and frequent fires could dramatically reduce tree cover in favor of shrub and grass cover; however, this mechanism was not accounted for in order to keep a straightforward comparison with the results of the previous DGVM version and to evaluate only the impact of new Arctic PFTs. This next step will require upgrading the new fire module implemented in ORCHIDEE (Yue et al., 2014) and adapting it for the behavior of shrubs and mosses. Disturbances at high latitude can indeed be the most important factor controlling vegetation distribution rather than climate warming (Myers-Smith et al., 2011).

The introduction of shrubs capable of outcompeting grasses for light directly reduces the extent of herbaceous vegetation in the model. Shrubs are able to grow further north than trees, despite having a similar critical survival temperature as boreal trees (section 2.4). This is due to the snow cover that reduces the impact of the minimum daily air temperature to which shrubs are exposed (Druel et al., 2017). Mosses are simulated in all boreal latitudes, but the fractional cover increases with latitude, and they become the largest vegetation cover north of 75°N. Quantitatively, this does not represent a large continental area, but it indicates their capacity to grow at high-latitude conditions, and this can have significant impacts on local soil moisture and heat conductivity (Beringer et al., 2001; Blok, Heijmans, et al., 2011; Chadburn et al., 2015b; Porada

et al., 2016). Moreover, the relatively low moss fractional cover in the simulations compared to the observations can be due to the limited representation of fire succession in this DGVM version, which leads to an underestimation of moss cover, given that mosses are the first low vegetation type to be established after a disturbance (Yuan et al., 2014).

The simulated tree extent is close to the satellite-based observations (Figure 3). The herbaceous cover is well represented, despite a partition between grasses and mosses that differs from present-day estimates (Figures 2 and 3). The simulated shrub coverage is, on average, too large, with regional fractional cover that can reach the maximum allowed in the model (0.95). However, the observed shrub coverage rarely exceeds 50% neither at the 2° spatial scale (CAVM Team, 2003; Druel et al., 2017; Frost & Epstein, 2014; Tape et al., 2006) nor at site level (section 3.3). This overrepresentation in the DGVM may be due to the shrub carbon allometry, which may favor too much the growth of the above ground carbon pools (compared to below ground ones) and therefore the spatial coverage. The allometry controls the dynamic of plant height, diameter and leaf area and thus its foliage-projected cover (see equation and Figure in Text S1). Potential improvements could be to reduce the maximum allowed shrub coverage (Figure 1) to a lower value than the one used for trees and/or to change the parameters of the allometry relationships (although the current values were derived from the literature and from calibration with in situ data as explained in Druel et al., 2017), in particular the maximum diameter. Such behavior can also be due to other processes not taken into account in this model version. For example, trampling by herbivores has already been considered as a key factor for the emergence of steppe-tundra vegetation (Zimov et al., 1995). In addition, the impact of wind speed through the modulation of the critical minimum temperature used in the calculation of the mortality could also play a significant role.

4.2. Arctic Vegetation Expansion at High Latitudes

The current increase in vegetation development toward high latitudes is becoming very well documented (e.g., Bonfils et al., 2012; Elmendorf et al., 2012; Frost & Epstein, 2014; Xu et al., 2013; Zhu et al., 2016) and is mainly attributed to climate change through temperature or water availability. Recent studies suggest that this expansion will probably continue in the future (Jiang et al., 2012; Zhang et al., 2013). Our model results suggest a future global decrease of bare soil and a considerable increase of tree cover (Figure 2). At high latitudes, the critical minimum temperature for tree survival is a key parameter in our model. Therefore, in our sensitivity tests to future warming, tree mortality linked to minimum winter temperatures is reduced, leading to an increased of tree cover. Mortality of broadleaved trees during spring frost events is also reduced in the model, despite the fact that warmer temperatures induce earlier season onset in spring with increasing frost exposure (Liu et al., 2018). Specifically, we observe a clear decrease of bare soil above 75°N, accompanied by an increase in the cover of mosses and grasses (Figure 5). Between 55°N and 75°N, the tree cover increases at the expense of shrubs, while mosses and grasses remain relatively constant. In both cases, there is an extension of global vegetation coverage to the north. Combined with a global increase of simulated LAI for each PFT in the three latitudinal bands (not shown), these results support the idea that there is a current Arctic greening and that it will increase over time.

It should be emphasized that the vegetation expansion mainly appears after the 2000s in the model, somewhat late compared to observations (Bonfils et al., 2012; Frost & Epstein, 2014; Jia et al., 2003; Sturm, Racine, et al., 2001; Zhu et al., 2016). However, the 1,000-year spin-up used in this study uses random meteorological forcing and CO_2 concentration from the years 1901 to 1950, during which a boreal temperature maximum was observed (Bengtsson et al., 2004), similar to temperatures in the late 1990s. Given that temperature and CO_2 are the main drivers of vegetation development in northern latitudes (Zhu et al., 2016), the distribution of the simulated vegetation at the end of the spin-up could already correspond or be close to the observed present-day vegetation distribution. Combined with the fact that the model NPP is highly sensitive to CO_2 and temperature, this spin-up procedure could partially bias the simulation of the recent evolution of vegetation cover. No expansion of vegetation was simulated from 1950 to 2000, whereas the evolution of the vegetation is significant from 2000 to 2100 in the climate warming sensitivity tests (around +5 °C in RCP 4.5 and +9 °C in RCP 8.5, in boreal latitudes).

Finally, the vegetation distribution expansion hides other aspects of ecosystem changes at high latitudes, such as the increase of productivity linked to precipitation and temperature (Figure 6). This could have substantial effects on carbon and water fluxes and associated climate feedbacks. It is therefore necessary to

combine changes on carbon fluxes and stocks (i.e., biomass and productivity) and evapotranspiration to assess the global impact of future vegetation evolution. Moreover, the structure of the vegetation coverage (type, density, ...) directly modifies the surface energy budget, impacting soil temperature and permafrost depth. Thus, all feedbacks linked to changes in vegetation distribution and properties should be studied with coupled soil temperature-hydrology models.

4.3. Shrub Distribution

We do not simulate a shrub expansion in the very high latitudes (Figures 2, 4, and 5), which is at odds with a growing number of recent observations (Blok, Schaepman-Strub, et al., 2011; Bonfils et al., 2012; Frost & Epstein, 2014; Myers-Smith et al., 2015; Zhang et al., 2013). This discrepancy could be explained by the minimal critical temperature that is used (which is the same as for trees), which mainly drives their northern distribution. There is a possibility that shrubs were already too far up north in the recent period simulations (Figure 5 and Table 1). Furthermore, additional simulations including warmer minimal critical temperatures for trees and shrubs (which will lead to increased mortality, see section 2.4) were tested; however, no substantial "shrubification" was simulated and significant differences between the present-day vegetation distribution and the observations were obtained (see Figure S3). An additional major contributing factor to explain the lack of shrub extension in northern latitudes (>65°N in Figure 5), where space is available for plant growth, is the protection of shrubs by snow (Druel et al., 2017). The associated mortality reduction can explain the higher proportion of shrubs at very high latitudes compared to trees. Due to the decrease in snow cover with global warming, or a discontinuous snow cover during winter as suggested by Gamm et al. (2017), the protection of shrubs diminishes. Thereby, the main advantage of shrubs against trees in boreal regions could be reduced, which in turn may limit shrub expansion under future climate change. It is also important to note that contrary to what could be expected with a global model, our simulations show no consistency across the five sites, although the observations show a systematic and significant trend. This may be due to a bias in the choice of the observation sites, chosen for the presence of shrubs, which are not necessarily representative of surrounding areas and thus of large-scale model grid cells.

Other processes potentially playing a role in the dynamic of vegetation distribution could be implemented or adapted from trees to shrubs with differential effects. For example, trees are more resistant to fire, but, with a higher regeneration rate, shrubs will have advantages in situations with successive fires. Also, the increase of the woody vegetation size makes trees more vulnerable to vessel freezing, cavitation (Hacke & Sperry, 2001), or wind throw. As a result, decreased shrub mortality combined with LAI increases (as shown in Table 1 and section 3.3) would lead to a shrub cover increase. Moreover, herbivores tend to inhibit climate-driven shrub expansion (Olofsson et al., 2009). Additionally, moisture availability or air temperature can impact shrub growth (Gamm et al., 2017; Myers-Smith et al., 2015; Young et al., 2016), and shrubs and trees have different requirements in terms of organic matter depth and active soil layer. Likewise, some processes developed in other versions of ORCHIDEE may also be critical, such as the nutrient availability requirement, the root profile depending on biomass, the plant succession, or the competition based on individuals (e.g., in Smith et al., 2011) instead of PFT fractional cover at grid scale. Moreover, in this study we considered only one type of boreal shrub. It would be conceivable, as for trees, to distinguish between different types of shrubs such as needleleaf and summergreen shrubs, as is done in JULES (Harper et al., 2016).

Conversely, the simulations show an increase of LAI (section 3.3), suggesting a climate-driven increase of shrub activity. Altogether, a decrease in shrub mortality (for the reasons explained above) would lead to a shrub cover increase. Some observations support also the possibility that no global or uniform shrub expansion would necessarily appear in the next decades with global warming. For example, a decline of shrub growth was observed in Greenland (Gamm et al., 2017). More generally, the sensitivity of shrub growth to climate change could locally be very heterogeneous as it also strongly depends on soil heterogeneity (fertility, water holding capacity, etc.) and the drivers are still poorly understood (Myers-Smith et al., 2015).

Finally, it could also be interesting to reconsider the idea of a continuous shrub expansion at northern latitudes. This expansion could be noncontinuous spatially and temporally, and may likely be undetectable in coarse-resolution (2°) simulations. Moreover, the observed shrub expansion could simply be a transient effect that actually masks a tree expansion. Indeed, the current implementation of shrubs in the model, very similar to the implementation of trees, and the large tree expansion simulated in northern latitudes suggest

that shrubs should be considered as "small trees," a step before becoming a tall tree in an environment where limitations for tree growth disappear.

5. Conclusions

We modeled the competition between different trees, grasses, shrubs, and mosses in the ORCHIDEE global dynamic vegetation model that previously only represented trees and grasses. The general principles of the original dynamic vegetation model are conserved, with trees outcompeting shrubs and both outcompeting grasses and mosses for light, and trees and shrubs being affected by mortality during cold winters. Here, shrubs are modeled like small trees (with new allometry relationship and parameters), except that they are protected by the winter snowpack and thus their winter mortality is lower than that of trees. Mosses are assigned a low photosynthetic rate, and their absence of roots makes them more sensitive than grasses to water stress episodes. The competitiveness of mosses stems from their opportunistic phenology as they can become dormant during dry periods and resume growth thereafter.

With these simple rules, the global dynamic vegetation model was shown to provide a reasonable representation of the present-day distribution of the vegetation types in the Northern Hemisphere, with an improvement compared to the previous dynamic model version. However, the model was not able to capture the observed fast rate of shrub area expansion at several Arctic sites during the last decades, although it does produce an increase of shrub LAI and productivity. The establishment or emergence of shrubs in ecosystems where they are endemic is probably strongly controlled by microscale effects like available thawed space and nutrients and by disturbances (such as fire succession) that are not modeled. Future projections of northern vegetation dynamics in response to climate and atmospheric CO_2 changes indicate a substantial Arctic vegetation expansion with a reduction of bare soil areas, as well as a continued greening, that is, increased LAI and productivity, with a higher impact on mosses in northern latitudes and on trees at intermediate latitudes. The decrease of bare soil fraction is continuous, but faster in the hottest scenario.

This study is part of the current effort to improve the quality of climate model predictions, for which vegetation dynamics are crucial, particularly in northern latitudes. The introduction of more detailed vegetation allows us to have a better representation of ecosystems and their complexity. Future research could focus on the effect of the different vegetation types including nonvascular plants or shrubs on soil temperature and on permafrost distribution, through their effect on soil thermal conductivity (water and carbon content), on winter snow insulation and on albedo differences and the associated feedbacks.

References

Baudena, M., Dekker, S. C., van Bodegom, P. M., Cuesta, B., Higgins, S. I., Lehsten, V., et al. (2015). Forests, savannas, and grasslands: bridging the knowledge gap between ecology and dynamic global vegetation models. *Biogeosciences*, *12*(6), 1833–1848. https://doi.org/10.5194/bg-12-1833-2015

Bengtsson, L., Semenov, V. A., & Johannessen, O. M. (2004). The early twentieth-century warming in the Arctic—A possible mechanism. *Journal of Climate*, *17*(20), 4045–4057. https://doi.org/10.1175/1520-0442(2004)017<4045:TETWIT>2.0.CO;2

Beringer, J., Lynch, A. H., Chapin, F. S., Mack, M., & Bonan, G. B. (2001). The representation of Arctic soils in the land surface model: The importance of mosses. *Journal of Climate*, *14*(15), 3324–3335. https://doi.org/10.1175/1520-0442(2001)014<3324:TROASI>2.0.CO;2

Betts, R. A. (2000). Offset of the potential carbon sink from boreal forestation by decreases in surface albedo. *Nature*, *408*(6809), 187–190. https://doi.org/10.1038/35041545

Blok, D., Heijmans, M. M. P. D., Schaepman-Strub, G., van Ruijven, J., Parmentier, F. J. W., Maximov, T. C., & Berendse, F. (2011). The cooling capacity of mosses: Controls on water and energy fluxes in a Siberian tundra site. *Ecosystems*, *14*(7), 1055–1065. https://doi.org/10.1007/s10021-011-9463-5

Blok, D., Schaepman-Strub, G., Bartholomeus, H., Heijmans, M. M. P. D., Maximov, T. C., & Berendse, F. (2011). The response of Arctic vegetation to the summer climate: Relation between shrub cover, NDVI, surface albedo and temperature. *Environmental Research Letters*, *6*(3), 35502. https://doi.org/10.1088/1748-9326/6/3/035502

Bonan, G. B. (1995). Land-atmosphere CO_2 exchange simulated by a land surface process model coupled to an atmospheric general circulation model. *Journal of Geophysical Research*, *100*(D2), 2817–2831. https://doi.org/10.1029/94JD02961

Bonfils, C. J. W., Phillips, T. J., Lawrence, D. M., Cameron-Smith, P., Riley, W. J., & Subin, Z. M. (2012). On the influence of shrub height and expansion on northern high latitude climate. *Environmental Research Letters*, *7*(1), 15503. https://doi.org/10.1088/1748-9326/7/1/015503

Boone, A. (2002). Description du schema de neige ISBA-ES (Explicit Snow), Note Cent. Meteo-FranceCNRM, (70), 53p.

Brovkin, V., Levis, S., Loutre, M.-F., Crucifix, M., Claussen, M., Ganopolski, A., et al. (2003). Stability analysis of the climate-vegetation system in the northern high latitudes. *Climatic Change*, *57*(1/2), 119–138. https://doi.org/10.1023/A:1022168609525

Bull, T. A. (1968). Expansion of leaf area per plant in field bean (Vicia fabia L.) as related to daily maximum temperature. *Journal of Applied Ecology*, *5*(1), 61–68. https://doi.org/10.2307/2401274

CAVM Team (2003). Circumpolar Arctic Vegetation Map, Conservation of Arctic Flora and Fauna (CAFF) Map No. 1. U.S. Fish and Wildlife Service, Anchorage, Alaska.

Chadburn, S., Burke, E., Essery, R., Boike, J., Langer, M., Heikenfeld, M., et al. (2015a). An improved representation of physical permafrost dynamics in the JULES land-surface model. *Geoscientific Model Development*, *8*(5), 1493–1508. https://doi.org/10.5194/gmd-8-1493-2015

Chadburn, S. E., Burke, E. J., Essery, R. L. H., Boike, J., Langer, M., Heikenfeld, M., et al. (2015b). Impact of model developments on present and future simulations of permafrost in a global land-surface model. *The Cryosphere*, *9*(4), 1505–1521. https://doi.org/10.5194/tc-9-1505-2015

Chapin, F. S., Mcguire, A. D., Randerson, J., Pielke, R., Baldocchi, D., Hobbie, S. E., et al. (2000). Arctic and boreal ecosystems of western North America as components of the climate system. *Global Change Biology*, *6*(S1), 211–223. https://doi.org/10.1046/j.1365-2486.2000.06022.x

Christensen, T., Jonasson, S., Callaghan, T., & Havström, M. (1999). On the potential CO2 release from tundra soils in a changing climate. *Applied Soil Ecology*, *11*(2–3), 127–134. https://doi.org/10.1016/S0929-1393(98)00146-2

Clark, D. B., Mercado, L. M., Sitch, S., Jones, C. D., Gedney, N., Best, M. J., et al. (2011). The Joint UK Land Environment Simulator (JULES), model description—Part 2: Carbon fluxes and vegetation dynamics. *Geoscientific Model Development*, *4*(3), 701–722. https://doi.org/10.5194/gmd-4-701-2011

Cook, B. I., Bonan, G. B., Levis, S., & Epstein, H. E. (2008). Rapid vegetation responses and feedbacks amplify climate model response to snow cover changes. *Climate Dynamics*, *30*(4), 391–406. https://doi.org/10.1007/s00382-007-0296-z

Cox, P. M., Betts, R. A., Jones, C. D., Spall, S. A., & Totterdell, I. J. (2000). Acceleration of global warming due to carbon-cycle feedbacks in a coupled climate model. *Nature*, *408*(6809), 184–187. https://doi.org/10.1038/35041539

Cresto Aleina, F., Runkle, B. R. K., Kleinen, T., Kutzbach, L., Schneider, J., & Brovkin, V. (2015). Modeling micro-topographic controls on boreal peatland hydrology and methane fluxes. *Biogeosciences*, *12*(19), 5689–5704. https://doi.org/10.5194/bg-12-5689-2015

Crucifix, M., & Loutre, F. (2002). Transient simulations over the last interglacial period (126–115 kyr BP): feedback and forcing analysis. *Climate Dynamics*, *19*(5–6), 417–433. https://doi.org/10.1007/s00382-002-0234-z

de Noblet, N. I., Prentice, I. C., Joussaume, S., Texier, D., Botta, A., & Haxeltine, A. (1996). Possible role of atmosphere-biosphere interactions in triggering the Last Glaciation. *Geophysical Research Letters*, *23*(22), 3191–3194. https://doi.org/10.1029/96GL03004

Druel, A., Peylin, P., Krinner, G., Ciais, P., Viovy, N., Peregon, A., et al. (2017). Towards a more detailed representation of high-latitude vegetation in the global land surface model ORCHIDEE (ORC-HL-VEGv1.0). *Geoscientific Model Development*, *10*(12), 4693–4722. https://doi.org/10.5194/gmd-10-4693-2017

Dufresne, J.-L., Foujols, M.-A., Denvil, S., Caubel, A., Marti, O., Aumont, O., et al. (2013). Climate change projections using the IPSL-CM5 Earth System Model: from CMIP3 to CMIP5. *Climate Dynamics*, *40*(9–10), 2123–2165. https://doi.org/10.1007/s00382-012-1636-1

Elmendorf, S. C., Henry, G. H. R., Hollister, R. D., Björk, R. G., Boulanger-Lapointe, N., Cooper, E. J., et al. (2012). Plot-scale evidence of tundra vegetation change and links to recent summer warming. *Nature Climate Change*, *2*(6), 453–457. https://doi.org/10.1038/nclimate1465

Epstein, H. E., Walker, M. D., Chapin, F. S., & Starfield, A. M. (2000). A transient, nutrient-based model of arctic plant community response to climatic warming. *Ecological Applications*, *10*(3), 824–841. https://doi.org/10.1890/1051-0761(2000)010[0824:ATNBMO]2.0.CO;2

Foley, J. A., Kutzbach, J. E., Coe, M. T., & Levis, S. (1994). Feedbacks between climate and boreal forests during the Holocene epoch. *Nature*, *371*(6492), 52–54. https://doi.org/10.1038/371052a0

Frost, G. V., & Epstein, H. E. (2014). Tall shrub and tree expansion in Siberian tundra ecotones since the 1960s. *Global Change Biology*, *20*(4), 1264–1277. https://doi.org/10.1111/gcb.12406

Gallimore, R. G., & Kutzbach, J. E. (1996). Role of orbitally induced changes in tundra area in the onset of glaciation. *Nature*, *381*(6582), 503–505. https://doi.org/10.1038/381503a0

Gamm, C. M., Sullivan, P. F., Buchwal, A., Dial, R. J., Young, A. B., Watts, D. A., et al. (2017). Declining growth of deciduous shrubs in the warming climate of continental western Greenland. *Journal of Ecology*, *106*(2), 640–654. https://doi.org/10.1111/1365-2745.12882

Gill, J. L. (2014). Ecological impacts of the late Quaternary megaherbivore extinctions. *The New Phytologist*, *201*(4), 1163–1169. https://doi.org/10.1111/nph.12576

Gouttevin, I., Krinner, G., Ciais, P., Polcher, J., & Legout, C. (2012). Multi-scale validation of a new soil freezing scheme for a land-surface model with physically-based hydrology. *The Cryosphere*, *6*(2), 407–430. https://doi.org/10.5194/tc-6-407-2012

Hacke, U. G., & Sperry, J. S. (2001). Functional and ecological xylem anatomy. *Perspectives in Plant Ecology, Evolution and Systematics*, *4*(2), 97–115. https://doi.org/10.1078/1433-8319-00017

Harper, A. B., Cox, P. M., Friedlingstein, P., Wiltshire, A. J., Jones, C. D., Sitch, S., et al. (2016). Improved representation of plant functional types and physiology in the Joint UK Land Environment Simulator (JULES v4.2) using plant trait information. *Geoscientific Model Development*, *9*(7), 2415–2440. https://doi.org/10.5194/gmd-9-2415-2016

Hartley, A. J., MacBean, N., Georgievski, G., & Bontemps, S. (2017). Uncertainty in plant functional type distributions and its impact on land surface models. *Remote Sensing of Environment*, *203*, 71–89. https://doi.org/10.1016/j.rse.2017.07.037

Haxeltine, A., & Prentice, I. C. (1996). BIOME3: An equilibrium terrestrial biosphere model based on ecophysiological constraints, resource availability, and competition among plant functional types. *Global Biogeochemical Cycles*, *10*(4), 693–709. https://doi.org/10.1029/96GB02344

Jia, G. J., Epstein, H. E., & Walker, D. A. (2003). Greening of arctic Alaska, 1981-2001: GREENING OF ARCTIC ALASKA, 1981-2001. *Geophysical Research Letters*, *30*(20), 2067. https://doi.org/10.1029/2003GL018268

Jiang, Y., Zhuang, Q., Schaphoff, S., Sitch, S., Sokolov, A., Kicklighter, D., & Melillo, J. (2012). Uncertainty analysis of vegetation distribution in the northern high latitudes during the 21st century with a dynamic vegetation model: Uncertainty analysis of vegetation distribution. *Ecology and Evolution*, *2*(3), 593–614. https://doi.org/10.1002/ece3.85

Kaplan, J. O., Bigelow, N. H., Prentice, I. C., Harrison, S. P., Bartlein, P. J., Christensen, T. R., et al. (2003). Climate change and Arctic ecosystems: 2. Modeling, paleodata-model comparisons, and future projections. *Journal of Geophysical Research*, *108*(D19), 8171. https://doi.org/10.1029/2002JD002559

Koven, C. D., Lawrence, D. M., & Riley, W. J. (2015). Permafrost carbon−climate feedback is sensitive to deep soil carbon decomposability but not deep soil nitrogen dynamics. *Proceedings of the National Academy of Sciences*. https://doi.org/10.1073/pnas.1415123112

Koven, C. D., Ringeval, B., Friedlingstein, P., Ciais, P., Cadule, P., Khvorostyanov, D., et al. (2011). Permafrost carbon-climate feedbacks accelerate global warming. *Proceedings of the National Academy of Sciences*, *108*(36), 14769–14774. https://doi.org/10.1073/pnas.1103910108

Krinner, G., Viovy, N., de Noblet-Ducoudré, N., Ogée, J., Polcher, J., Friedlingstein, P., et al. (2005). A dynamic global vegetation model for studies of the coupled atmosphere-biosphere system: DVGM FOR COUPLED CLIMATE STUDIES. *Global Biogeochemical Cycles*, *19*, GB1015. https://doi.org/10.1029/2003GB002199

Lane, D. R., Coffin, D. P., & Lauenroth, W. K. (2000). Changes in grassland canopy structure across a precipitation gradient. *Journal of Vegetation Science*, *11*(3), 359–368. https://doi.org/10.2307/3236628

Lawrence, D. M., & Swenson, S. C. (2011). Permafrost response to increasing Arctic shrub abundance depends on the relative influence of shrubs on local soil cooling versus large-scale climate warming. *Environmental Research Letters*, *6*(4), 45504. https://doi.org/10.1088/1748-9326/6/4/045504

Liston, G. E., Mcfadden, J. P., Sturm, M., & Pielke, R. A. (2002). Modelled changes in arctic tundra snow, energy and moisture fluxes due to increased shrubs. *Global Change Biology*, *8*(1), 17–32. https://doi.org/10.1046/j.1354-1013.2001.00416.x

Liu, Q., Piao, S., Janssens, I. A., Fu, Y., Peng, S., Lian, X., et al. (2018). Extension of the growing season increases vegetation exposure to frost. *Nature Communications*, *9*(1), 426. https://doi.org/10.1038/s41467-017-02690-y

Loranty, M. M., Berner, L. T., Goetz, S. J., Jin, Y., & Randerson, J. T. (2014). Vegetation controls on northern high latitude snow-albedo feedback: Observations and CMIP5 model simulations. *Global Change Biology*, *20*(2), 594–606. https://doi.org/10.1111/gcb.12391

Loveland, T. R., Reed, B. C., Brown, J. F., Ohlen, D. O., Zhu, Z., Yang, L., & Merchant, J. W. (2000). Development of a global land cover characteristics database and IGBP DISCover from 1 km AVHRR data. *International Journal of Remote Sensing*, *21*(6–7), 1303–1330. https://doi.org/10.1080/014311600210191

Luus, K. A., Gel, Y., Lin, J. C., Kelly, R. E. J., & Duguay, C. R. (2013). Pan-Arctic linkages between snow accumulation and growing-season air temperature, soil moisture and vegetation. *Biogeosciences*, *10*(11), 7575–7597. https://doi.org/10.5194/bg-10-7575-2013

Macias-Fauria, M., Forbes, B. C., Zetterberg, P., & Kumpula, T. (2012). Eurasian Arctic greening reveals teleconnections and the potential for structurally novel ecosystems. *Nature Climate Change*, *2*(8), 613–618. https://doi.org/10.1038/nclimate1558

Meissner, K. J., Weaver, A. J., Matthews, H. D., & Cox, P. M. (2003). The role of land surface dynamics in glacial inception: a study with the UVic Earth System Model. *Climate Dynamics*, *21*(7–8), 515–537. https://doi.org/10.1007/s00382-003-0352-2

Moss, R. H., Edmonds, J. A., Hibbard, K. A., Manning, M. R., Rose, S. K., van Vuuren, D. P., et al. (2010). The next generation of scenarios for climate change research and assessment. *Nature*, *463*(7282), 747–756. https://doi.org/10.1038/nature08823

Myers-Smith, I. H., Elmendorf, S. C., Beck, P. S. A., Wilmking, M., Hallinger, M., Blok, D., et al. (2015). Climate sensitivity of shrub growth across the tundra biome. *Nature Climate Change*, *5*(9), 887–891. https://doi.org/10.1038/nclimate2697

Myers-Smith, I. H., Hik, D. S., Kennedy, C., Cooley, D., Johnstone, J. F., Kenney, A. J., & Krebs, C. J. (2011). Expansion of canopy-forming willows over the twentieth century on Herschel Island, Yukon Territory, Canada. *Ambio*, *40*(6), 610–623. https://doi.org/10.1007/s13280-011-0168-y

Naito, A. T., & Cairns, D. M. (2015). Patterns of shrub expansion in Alaskan arctic river corridors suggest phase transition. *Ecology and Evolution*, *5*(1), 87–101. https://doi.org/10.1002/ece3.1341

Oki, T., & Kanae, S. (2006). Global hydrological cycles and world water resources. *Science*, *313*(5790), 1068–1072. https://doi.org/10.1126/science.1128845

Oleson, K., Lawrence, D., Bonan, G., Drewniak, B., Huang, M., Koven, C., et al. (2013). Technical description of version 4.5 of the Community Land Model (CLM), doi:https://doi.org/10.5065/D6RR1W7M.

Olofsson, J., Oksanen, L., Callaghan, T., Hulme, P. E., Oksanen, T., & Suominen, O. (2009). Herbivores inhibit climate-driven shrub expansion on the tundra: Herbivores inhibit shrub expansion. *Global Change Biology*, *15*(11), 2681–2693. https://doi.org/10.1111/j.1365-2486.2009.01935.x

Öztürk, M., Bolat, İ., & Ergün, A. (2015). Influence of air–soil temperature on leaf expansion and LAI of Carpinus betulus trees in a temperate urban forest patch. *Agricultural and Forest Meteorology*, *200*, 185–191. https://doi.org/10.1016/j.agrformet.2014.09.014

Pachzelt, A., Forrest, M., Rammig, A., Higgins, S. I., & Hickler, T. (2015). Potential impact of large ungulate grazers on African vegetation, carbon storage and fire regimes: Grazer impacts on African savannas. *Global Ecology and Biogeography*, *24*(9), 991–1002. https://doi.org/10.1111/geb.12313

Pearson, R. G., Phillips, S. J., Loranty, M. M., Beck, P. S. A., Damoulas, T., Knight, S. J., & Goetz, S. J. (2013). Shifts in Arctic vegetation and associated feedbacks under climate change. *Nature Climate Change*, *3*(7), 673–677. https://doi.org/10.1038/nclimate1858

Piao, S., Friedlingstein, P., Ciais, P., Zhou, L., & Chen, A. (2006). Effect of climate and CO₂ changes on the greening of the Northern Hemisphere over the past two decades. *Geophysical Research Letters*, *33*, L23402. https://doi.org/10.1029/2006GL028205

Porada, P., Ekici, A., & Beer, C. (2016). Effects of bryophyte and lichen cover on permafrost soil temperature at large scale. *The Cryosphere*, *10*(5), 2291–2315. https://doi.org/10.5194/tc-10-2291-2016

Porada, P., Weber, B., Elbert, W., Pöschl, U., & Kleidon, A. (2013). Estimating global carbon uptake by lichens and bryophytes with a process-based model. *Biogeosciences*, *10*(11), 6989–7033. https://doi.org/10.5194/bg-10-6989-2013

Prentice, I. C., Cramer, W., Harrison, S. P., Leemans, R., Monserud, R. A., & Solomon, A. M. (1992). Special Paper: A global biome model based on plant physiology and dominance, soil properties and climate. *Journal of Biogeography*, *19*(2), 117. https://doi.org/10.2307/2845499

Prentice, I. C., & Leemans, R. (1990). Pattern and process and the dynamics of forest structure: A simulation approach. *Journal of Ecology*, *78*(2), 340. https://doi.org/10.2307/2261116

Quillet, A., Peng, C., & Garneau, M. (2010). Toward dynamic global vegetation models for simulating vegetation–climate interactions and feedbacks: Recent developments, limitations, and future challenges. *Environmental Reviews*, *18*, 333–353. https://doi.org/10.1139/A10-016

Rinke, A., Kuhry, P., & Dethloff, K. (2008). Importance of a soil organic layer for Arctic climate: A sensitivity study with an Arctic RCM. *Geophysical Research Letters*, *35*, L13709. https://doi.org/10.1029/2008GL034052

Schimel, D. S. (1995). Terrestrial ecosystems and the carbon cycle. *Global Change Biology*, *1*(1), 77–91. https://doi.org/10.1111/j.1365-2486.1995.tb00008.x

Sinclair, A. R. E., Mduma, S. A. R., Hopcraft, J. G. C., Fryxell, J. M., Hilborn, R., & Thirgood, S. (2007). Long-term ecosystem dynamics in the Serengeti: Lessons for conservation. *Conservation Biology*, *21*(3), 580–590. https://doi.org/10.1111/j.1523-1739.2007.00699.x

Sitch, S., Smith, B., Prentice, I. C., Arneth, A., Bondeau, A., Cramer, W., et al. (2003). Evaluation of ecosystem dynamics, plant geography and terrestrial carbon cycling in the LPJ dynamic global vegetation model. *Global Change Biology*, *9*(2), 161–185. https://doi.org/10.1046/j.1365-2486.2003.00569.x

Smith, B., Samuelsson, P., Wramneby, A., & Rummukainen, M. (2011). A model of the coupled dynamics of climate, vegetation and terrestrial ecosystem biogeochemistry for regional applications: Regional climate-vegetation-biogeochemistry model. *Tellus A*, *63*(1), 87–106. https://doi.org/10.1111/j.1600-0870.2010.00477.x

Sturm, M., Holmgren, J., McFadden, J. P., Liston, G. E., Chapin, F. S., & Racine, C. H. (2001). Snow–shrub interactions in Arctic tundra: A hypothesis with climatic implications. *Journal of Climate*, *14*(3), 336–344. https://doi.org/10.1175/1520-0442(2001)014<0336:SSIIAT>2.0.CO;2

Sturm, M., Racine, C., & Tape, K. (2001). Increasing shrub abundance in the Arctic. *Nature*, *411*(6837), 546–547. https://doi.org/10.1038/35079180

Tape, K., Sturm, M., & Racine, C. (2006). The evidence for shrub expansion in Northern Alaska and the Pan-Arctic. *Global Change Biology*, *12*(4), 686–702. https://doi.org/10.1111/j.1365-2486.2006.01128.x

Thonicke, K., Venevsky, S., Sitch, S., & Cramer, W. (2008). The role of fire disturbance for global vegetation dynamics: coupling fire into a dynamic global vegetation model: Fire disturbance and global vegetation dynamics. *Global Ecology and Biogeography*, *10*(6), 661–677. https://doi.org/10.1046/j.1466-822X.2001.00175.x

Trenberth, K. E., Fasullo, J. T., & Kiehl, J. (2009). Earth's global energy budget. *Bulletin of the American Meteorological Society*, *90*(3), 311–324. https://doi.org/10.1175/2008BAMS2634.1

Viovy, N. (2015). Forcing ORCHIDEE: 1.1 CRU-NCEP, Forching Orchid. [online] Available from: http://forge.ipsl.jussieu.fr/orchidee/wiki/Documentation/Forcings#a1.1CRU-NCEP (Accessed 9 June 2016).

Wang, T., Ottlé, C., Boone, A., Ciais, P., Brun, E., Morin, S., et al. (2013). Evaluation of an improved intermediate complexity snow scheme in the ORCHIDEE land surface model: ORCHIDEE snow model evaluation. *Journal of Geophysical Research: Atmospheres*, *118*, 6064–6079. https://doi.org/10.1002/jgrd.50395

Wei, Y., Liu, S., Huntzinger, D. N., Michalak, A. M., Viovy, N., Post, W. M., et al. (2014). The North American Carbon Program Multi-scale Synthesis and Terrestrial Model Intercomparison Project—Part 2: Environmental driver data. *Geoscientific Model Development*, *7*(6), 2875–2893. https://doi.org/10.5194/gmd-7-2875-2014

Xu, L., Myneni, R. B., Chapin, F. S. III, Callaghan, T. V., Pinzon, J. E., Tucker, C. J., et al. (2013). Temperature and vegetation seasonality diminishment over northern lands. *Nature Climate Change*, *3*(6), 581–586. https://doi.org/10.1038/nclimate1836

Yin, X., & Struik, P. C. (2009). C3 and C4 photosynthesis models: An overview from the perspective of crop modelling. *NJAS - Wageningen Journal of Life Sciences*, *57*(1), 27–38. https://doi.org/10.1016/j.njas.2009.07.001

Young, A. B., Watts, D. A., Taylor, A. H., & Post, E. (2016). Species and site differences influence climate-shrub growth responses in West Greenland. *Dendrochronologia*, *37*, 69–78. https://doi.org/10.1016/j.dendro.2015.12.007

Yuan, W., Liu, S., Dong, W., Liang, S., Zhao, S., Chen, J., et al. (2014). Differentiating moss from higher plants is critical in studying the carbon cycle of the boreal biome. *Nature Communications*, *5*(1). https://doi.org/10.1038/ncomms5270

Yue, C., Ciais, P., Cadule, P., Thonicke, K., Archibald, S., Poulter, B., et al. (2014). Modelling the role of fires in the terrestrial carbon balance by incorporating SPITFIRE into the global vegetation model ORCHIDEE – Part 1: simulating historical global burned area and fire regimes. *Geoscientific Model Development*, *7*(6), 2747–2767. https://doi.org/10.5194/gmd-7-2747-2014

Zhang, J.-H., Fu, C.-B., Yan, X.-D., Seita, E., & Hiroshi, K. (2002). A global respondence analysis of LAI versus surface air temperature and precipitation variations. *Chinese Journal of Geophysics*, *45*(5), 662–669. https://doi.org/10.1002/cjg2.280

Zhang, W., Miller, P. A., Smith, B., Wania, R., Koenigk, T., & Döscher, R. (2013). Tundra shrubification and tree-line advance amplify arctic climate warming: Results from an individual-based dynamic vegetation model. *Environmental Research Letters*, *8*(3), 34023. https://doi.org/10.1088/1748-9326/8/3/034023

Zhu, D., Peng, S. S., Ciais, P., Viovy, N., Druel, A., Kageyama, M., et al. (2015). Improving the dynamics of Northern Hemisphere high-latitude vegetation in the ORCHIDEE ecosystem model. *Geoscientific Model Development*, *8*(7), 2263–2283. https://doi.org/10.5194/gmd-8-2263-2015

Zhu, Z., Piao, S., Myneni, R. B., Huang, M., Zeng, Z., Canadell, J. G., et al. (2016). Greening of the Earth and its drivers. *Nature Climate Change*, *6*(8), 791–795. https://doi.org/10.1038/nclimate3004

Zimov, S. A., Chuprynin, V. I., Oreshko, A. P., Chapin, F. S., Reynolds, J. F., & Chapin, M. C. (1995). Steppe-tundra transition: A herbivore-driven biome shift at the end of the Pleistocene. *The American Naturalist*, *146*(5), 765–794. https://doi.org/10.1086/285824

References From the Supporting Information

Aiba, S.-I., & Kohyama, T. (1996). Tree Species Stratification in relation to allometry and demography in a warm-temperate rain forest. *Journal of Ecology*, *84*(2), 207–218. https://doi.org/10.2307/2261356

Bentley, J. R., Seegrist, D. & Blakeman, D. A. (1970). A technique for sampling low shrub vegetation, by cromwn volume classes, Res Note PSW-RN-215 Berkeley CA US Dep. Agric. For. Serv. Pac. Southwest For. Range Exp. Stn., 12p.

Lufafa, A., Diédhiou, I., Ndiaye, N. A. S., Séné, M., Kizito, F., Dick, R. P., & Noller, J. S. (2009). Allometric relationships and peak-season community biomass stocks of native shrubs in Senegal's Peanut Basin. *Journal of Arid Environments*, *73*(3), 260–266. https://doi.org/10.1016/j.jaridenv.2008.09.020

Martínez, A. J., & López-Portillo, J. (2003). Allometry of *Prosopis glandulosa* var. *torreyana* along a topographic gradient in the Chihuahuan desert. *Journal of Vegetation Science*, *14*(1), 111–120. https://doi.org/10.1111/j.1654-1103.2003.tb02133.x

Smith, B., Prentice, I. C., & Sykes, M. T. (2001). Representation of vegetation dynamics in the modelling of terrestrial ecosystems: Comparing two contrasting approaches within European climate space: Vegetation dynamics in ecosystem models. *Global Ecology and Biogeography*, *10*(6), 621–637. https://doi.org/10.1046/j.1466-822X.2001.t01-1-00256.x